Fluorescent indicators for Ca^{2+} based on green fluorescent proteins and calmodulin

Atsushi Miyawaki*, Juan Llopis*, Roger Heim*†, J. Michael McCaffery‡, Joseph A. Adams§, Mitsuhiko Ikura‖, & Roger Y. Tsien*†

** Department of Pharmacology, † Howard Hughes Medical Institute, and ‡ Division of Cellular and Molecular Medicine, University of California, San Diego, La Jolla, California 92093-0647, USA*
§ Department of Chemistry, San Diego State University, San Diego, California 92182-1030, USA
‖ Division of Molecular and Structural Biology, Ontario Cancer Institute, and Department of Medical Biophysics, University of Toronto, Toronto M5G 2M9, Canada, and Center for Tsukuba Advanced Research Alliance, University of Tsukuba, Tsukuba 305, Japan

Important Ca^{2+} signals in the cytosol and organelles are often extremely localized and hard to measure. To overcome this problem we have constructed new fluorescent indicators for Ca^{2+} that are genetically encoded without cofactors and are targetable to specific intracellular locations. We have dubbed these fluorescent indicators 'cameleons'. They consist of tandem fusions of a blue- or cyan-emitting mutant of the green fluorescent protein (GFP)[1,2], calmodulin[3–5], the calmodulin-binding peptide M13 (ref. 6), and an enhanced green- or yellow-emitting GFP[7–9]. Binding of Ca^{2+} makes calmodulin wrap around the M13 domain, increasing the fluorescence resonance energy transfer (FRET) between the flanking GFPs[2]. Calmodulin mutations can tune the Ca^{2+} affinities to measure free Ca^{2+} concentrations in the range 10^{-8} to 10^{-2} M. We have visualized free Ca^{2+} dynamics in the cytosol, nucleus and endoplasmic reticulum of single HeLa cells transfected with complementary DNAs encoding chimaeras bearing appropriate localization signals. Ca^{2+} concentration in the endoplasmic reticulum of individual cells ranged from 60 to 400 μM at rest, and 1 to 50 μM after Ca^{2+} mobilization. FRET is also an indicator of the reversible *inter*molecular association of cyan-GFP-labelled calmodulin with yellow-GFP-labelled M13. Thus FRET between GFP mutants can monitor localized Ca^{2+} signals and protein heterodimerization in individual live cells.

Cytosolic and organellar free Ca^{2+} concentrations are among the most important and dynamic intracellular signals, and are usually measured using synthetic fluorescent chelators[10–13] or recombinant aequorin[14,15]. The chelators are easily imaged but are difficult to target precisely to specific intracellular locations, whereas aequorin is easily targeted but requires the incorporation of coelenterazine, is irreversibly consumed by Ca^{2+}, and is very difficult to image because its luminescence produces less than one photon per molecule. To combine the brightness of fluorescent indicators with the targetability of a biosynthetic indicator, we have used GFP, a spontaneously fluorescent protein from the jellyfish *Aequorea victoria*. Its cDNA can be concatenated with those encoding many other proteins, and the resulting fusion proteins are usually fluorescent and often preserve the biochemical functions and cellular localizations of the partner proteins. Mutagenesis has produced GFP mutants with shifted wavelengths of excitation or emission[1,2,7,9] that can serve as donors and acceptors for FRET. FRET is a non-destructive spectroscopic method that can monitor the proximity and relative angular orientation of fluorophores in living cells. The donor and acceptor fluorophores can be entirely separate or

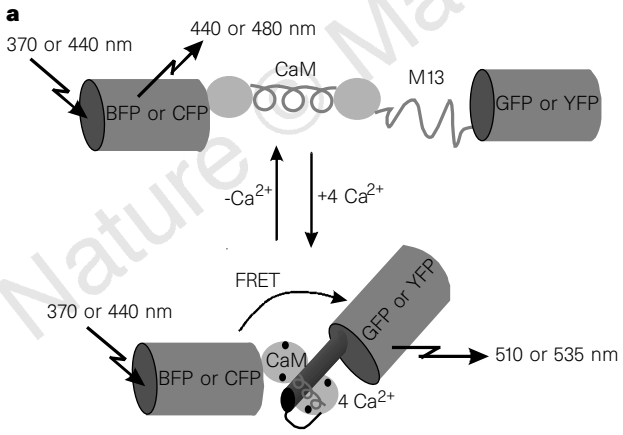

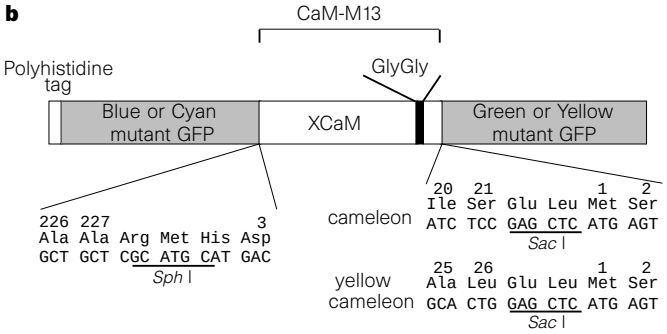

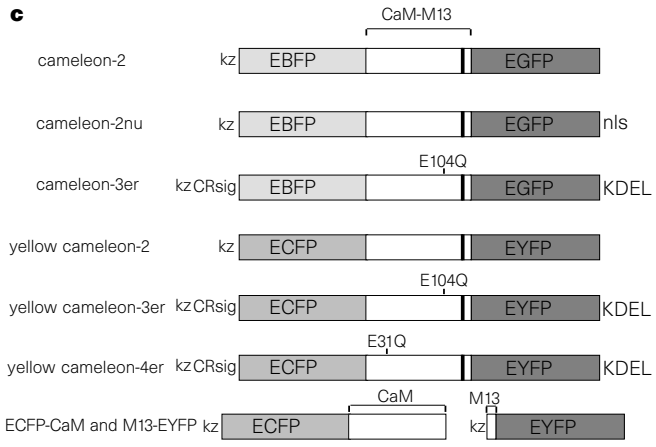

Figure 1 Schematic structures and sequences of cameleons. **a**, Scheme showing how FRET between GFPs can measure Ca^{2+}. The GFPs are drawn as simple rigid cylinders, reflecting their crystal structures[9]. Schematic structures of calmodulin (CaM) without Ca^{2+}, disordered unbound M13, and the Ca^{2+}–calmodulin–M13 complex are derived from crystallography[4], NMR[6] and modelling[16], but the relative orientations of the GFPs are unknown. **b**, Domain structure of cameleons expressed in bacteria for *in vitro* characterization, showing sequences of the boundaries between the donor GFP and *Xenopus* calmodulin (XCaM) and between M13 and the acceptor GFP. **c**, Consitition of cameleons for expression and imaging in mammalian cells. CRsig, calreticulin signal sequence, MLLSVPLLLGLLGLAAAD[24]; nls, nuclear localizaiton signal, PKKKRKVEDA; KDEL, ER retention signal[24]; kz, Kozak consensus sequence for optimal translational iniitation in mammalian cells[28]. The significant mutations in the four GFPs are: EBFP, F64L/Y66H/Y145[2]; EGFP, F64L/S65T[8]; ECFP, F64L/S65T/Y66W/N146I/M153T/V163A/N212K[2]; and EYFP, S65G/S72A/T203Y[9].

attached to the same macromolecule. In the latter case, ligand-induced conformational changes might be monitored by FRET if the amino and carboxy termini of the binding protein are fused to a donor and acceptor GFP. This approach has several advantages over the usual covalent labelling with fluorescent probes. First, the indicator is generated *in situ* by gene transfer into the cells or organisms, obviating large-scale expression, purification, labelling and microinjection of recombinant proteins that must be soluble. Second, the sites of fusions are defined exactly, giving a molecularly homogenous product without the use of elaborate protein chemistry. Third, the chromophore of GFP is fixed in the protein[9]. If the GFP donor and acceptor are rigidly fused to a host protein, minor changes in the relative orientation of the ends of the latter would alter FRET. In contrast, most conventional fluorescent labels are attached by flexible linkers that at least partly decouple the fluorophore orientation from that of the protein to which it is attached.

Many effects of Ca^{2+} in cells are mediated by the binding of Ca^{2+} to calmodulin, which causes calmodulin to bind and activate target proteins[3]. Based on the nuclear magnetic resonance solution structure of calmodulin bound to M13, the 26-residue calmodulin-binding peptide of myosin light-chain kinase[6], the C terminus of calmodulin has been fused to the M13 by means of a Gly-Gly spacer[16]. Ca^{2+} binding switched the resulting hybrid protein (calmodulin–M13) from a dumb-bell-like extended form to a compact globular form similar to the calmodulin–M13 intermolecular complex. We therefore sandwiched the calmodulin–M13 fusion between a blue (Y66H/Y145F)[2] and a green (S65T)[7] GFP mutant to construct a Ca^{2+} indicator (Fig. 1a). The amino-acid sequences of the boundary regions between the calmodulin–M13 hybrid and GFPs proved critical to the optimization of protein folding and the Ca^{2+} sensitivity of FRET. Numerous deletions, insertions and amino-acid substitutions were tested; the best splice sequences found are shown in Fig. 1b. The prototype fusion protein was efficiently expressed and folded in bacteria and increased its ratio of ultraviolet-excited 510:445 nm emissions by 70% upon binding Ca^{2+} (Fig. 2a). The decrease in blue and increase in green emission indicated that Ca^{2+} increased the efficiency of FRET from Y66H/Y145F to S65T, consistent with the expected decrease in distance between the two ends of the protein. The Ca^{2+} response was fully reversible upon chelation of Ca^{2+}. We have called this calmodulin-based indicator 'cameleon-1', because it readily changes colour and retracts and extends a long tongue (M13) into and out of the mouth of the calmodulin, often abbreviated CaM. Mg^{2+}, pH and ionic strength did not alter the emission spectra of either the Ca^{2+}-saturated or Ca^{2+}-unsaturated forms (data not shown), in accord with the typical high specificity of calmodulin for Ca^{2+} (ref. 5). Cameleon-1 was not affected by hydrophobic proteins, such as bovine serum albumin. Isolated calmodulin saturated with Ca^{2+} becomes sticky with hydrophobic amino acids exposed to the surface. The calmodulin in cameleon-1, however, seems to interact preferentially with its intramolecularly adjacent M13 peptide. Such a self-contained system should minimize the possibility that the protein might interact with endogenous calmodulin-binding sequences in eukaryotic cells.

The original calmodulin–M13 hybrid protein without GFPs displayed a biphasic Ca^{2+} binding with two dissociation constants,

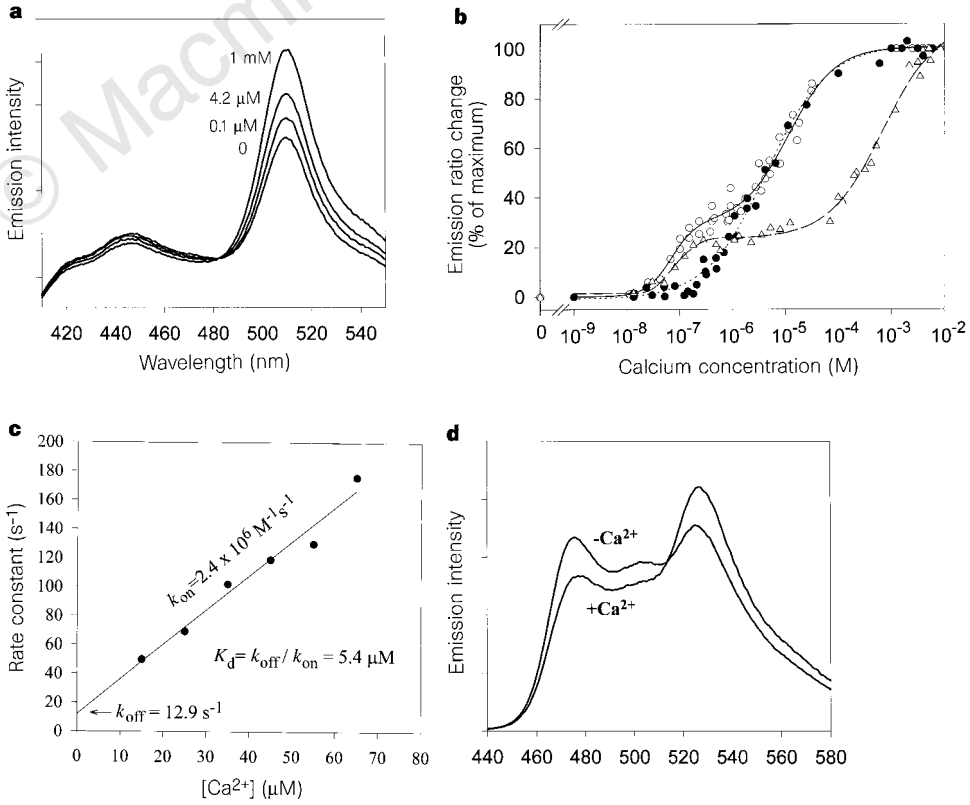

Figure 2 Properties of cameleons *in vitro*. **a**, Emission spectra of cameleon-1 (excited at 380 nm) at the indicated free Ca^{2+} values at pH 7.47. **b**, Ca^{2+} titration curves of cameleon-1 (open circles), cameleon-1/E104Q (filled circles), and cameleon-1/E31Q (open triangles), combining 5 independent experiments using Ca^{2+}/EGTA and Ca^{2+}/HEEDTA systems[10] below 10^{-5} M free Ca^{2+} and unbuffered Ca^{2+} above. The changes in emission ratio (510 to 445 nm) were normalized to the effects of full Ca^{2+} saturation, which were 60–80% increases in ratio over the values at zero Ca^{2+}. The fitted curves correspond to the apparent dissociation constants and Hill coefficients given in the text. **c**, Relaxation rate constants, k_{obs} ($= k_{on}[Ca^{2+}] + k_{off}$), for reaction of cameleon-1/E104Q with Ca^{2+}; k_{on} and k_{off} are the association and dissociation rate constants. **d**, Emission spectrum of yellow cameleon-2 *in vitro*, excited at 432 nm, at zero and saturating Ca^{2+}.

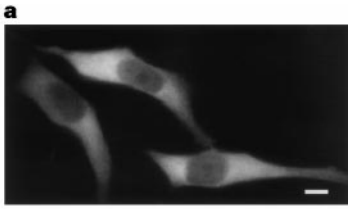

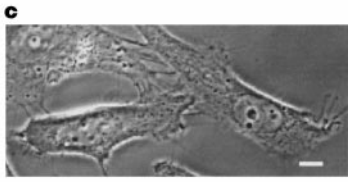

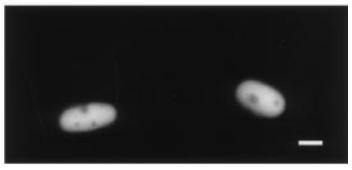

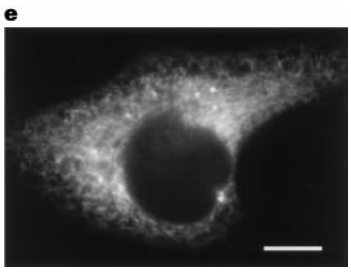

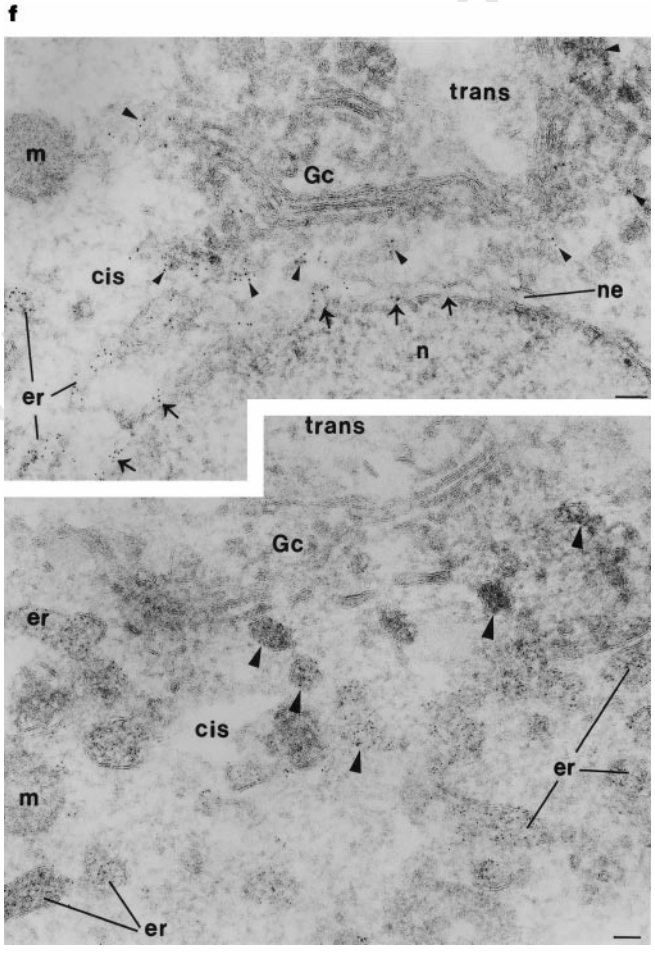

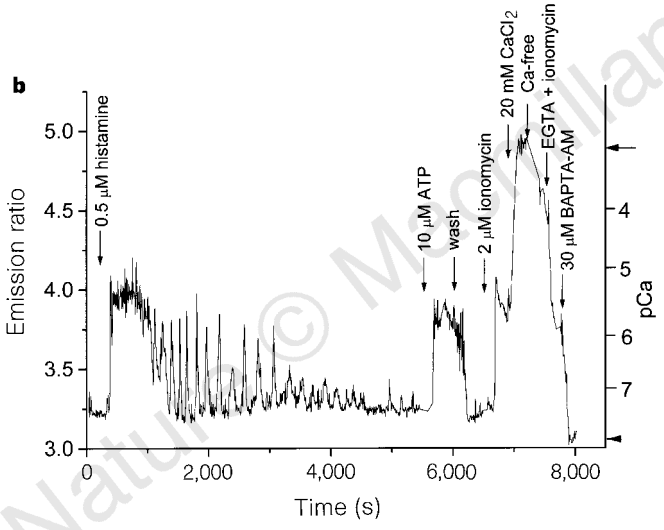

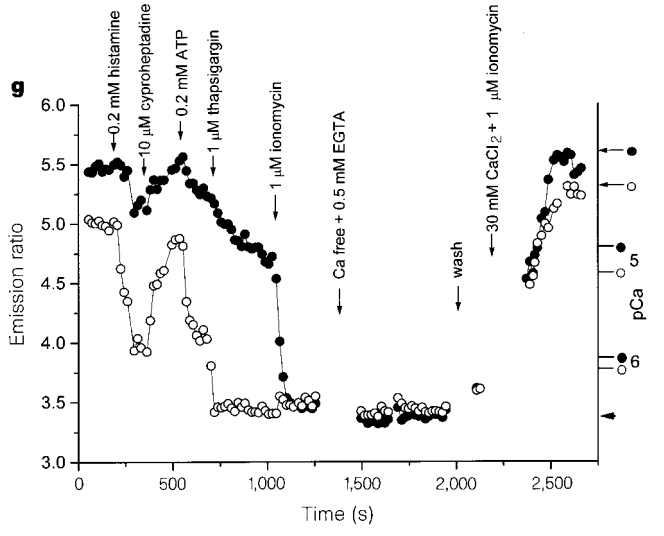

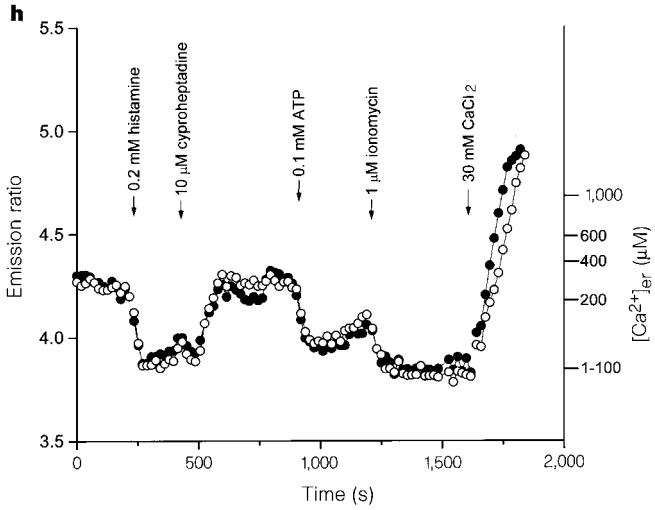

Figure 3 Imaging of cameleons in HeLa cells. **a**, Fluorescence image (440 ± 10 nm excitation, 535 ± 12.5 nm emission) of yellow cameleon-2 shows cytosolic localizaiton in HeLa cells. Scale bar, 10 μm in all fluorescence images. **b**, Ratios of 535 ± 12.5 nm to 480 ± 15 nm emissions from yellow cameleon-2 in the cytoplasm of the leftmost cell of **a**, monitored every 7 s by digital imaging microscopy. The ratios were calibrated in terms of absolute pCa on the right-hand ordinate axis, using R_{min} (arrowhead) and R_{max} (arrow) determined *in situ*. 'Ca^{2+} free' indicates medium containing 0.5 mM $MgCl_2$. **c**, **d**, Matched phase-contrast and fluorescence (480 ± 15 nm excitation, 535 ± 22.5 nm emission) images of two HeLa cells showing cameleon-2nu localized to the nuclei. **e**, Fluorescence image of yellow cameleon-3er, taken as in **a**. The same reticular pattern of fluorescence was observed for yellow cameleon-4er. **f**, Immunogold localizaiton of cameleon-3er in ultrathin cryosections using a polyclonal antibody against GFP. The cameleon-3er was abundant in the ER (er), nuclear envelope (ne and arrows) and intermediate compartment (arrowheads), but absent from the *cis*-most Golgi cisternae (Gc), mitochondria (m) and nucleus (n). 'Cis' and 'trans' show the orientation of the Golgi stack but do not mark specific structures. Scale bars, 0.1 μm. **g**, The 535 to 480 nm emission ratios from yellow cameleon-3er in two cells. The right-hand ordinate gives R_{min} (arrowhead), R_{max} (arrows) and pCa calibrations for each cell. **h**, Analogous emission ratios from yellow cameleon-4er in two cells. The right-hand ordinate calibrates $[Ca^{2+}]_{er}$.

2 μM and 80 nM, resulting from independent Ca^{2+} binding to the N- and C-terminal domains of calmodulin, respectively[16]. The emission ratio of cameleon-1 has a similar biphasic Ca^{2+} dependency (Fig. 2b, open circles) with apparent dissociation constants (K'_d) of 11 μM and 70 nM, and Hill coefficients (n) of 1.0 and 1.8, respectively. Therefore cameleon-1 can report a very wide range of Ca^{2+} concentration, from $<10^{-7}$ to $>10^{-4}$ M. Many site-directed mutations have been studied for their effects on the Ca^{2+} binding and Ca^{2+}-induced conformational changes of calmodulin[17,18]. Mutation of the conserved bidentate glutamic acid (E104) at position 12 of the third Ca^{2+}-binding loop to glutamine (Q) eliminated the high-affinity component of the Ca^{2+} response (Fig. 2b, filled circles). The resulting monophasic response (K'_d, 4.4 μM; n, 0.76) corresponded fairly closely to the low-affinity component of the cameleon-1 response. An analogous mutation in the first Ca^{2+}-binding loop (E31Q) resulted in a large rightward shift of the low-affinity component of cameleon-1, without affecting the high-affinity component (Fig. 2b, triangles). Cameleon-1/E31Q showed a biphasic response (K'_d, 83 nM and 700 μM; n, 1.5 and 0.87. Much more tuning of Ca^{2+} affinities for particular applications should be possible.

Because cameleon-1/E104Q had the simplest Ca^{2+}-response curve, it was chosen for initial explorations of Ca^{2+}-binding kinetics by stopped-flow measurements of the acceptor S65T emission after rapid mixing with Ca^{2+}. The approach to equilibrium was reasonably exponential, and the inverse time constants were a linear function of free $[Ca^{2+}]$, as expected for simple 1 : 1 binding (Fig. 2c). The association and dissociation rate constants correspond to the slope and intercept of the linear plot and were $(2.4 \pm 0.2) \times 10^6\ M^{-1}\ s^{-1}$ and $13 \pm 9\ s^{-1}$, in 100 mM KCl at 25 °C. Their ratio is 5.4 μM, which is consistent with the apparent dissociation constant (4.4 μM) independently derived from equilibrium measurements (Fig. 2b). The dissociation rate is similar to that ($12 \pm 2\ s^{-1}$) for calmodulin and M13 without the GFPs[19], so the GFPs do not perturb the dissociation even though they are much larger than the interacting calmodulin and M13 domains.

Can cameleons work as Ca^{2+} indicators in mammalian cells? Initial transfections with the gene encoding cameleon-1 in the pcDNA3 vector (with a cytomegalovirus promoter) gave inadequate fluorescence because the blue was not bright enough. The simplest remedy was to introduce mammalian codon bias and mutate Phe 64 to Leu, which improves expression and folding of GFPs at 37 °C without greatly affecting the spectra of the final well-folded molecules[8,20]. The resulting enhanced blue and green fluorescent proteins ('EBFP' and EGFP, respectively) fused to calmodulin–M13 constituted cameleon-2 (Fig. 1c), which indeed greatly improved mammalian cell expression. However, an even better approach for single-cell imaging proved to be replacement of the EBFP and EGFP by similarly enhanced cyan and yellow fluorescent mutants, 'ECFP' and 'EYFP', respectively (Fig. 1c). ECFP contains Trp at residue 66 in place of the His of EBFP and Tyr of EGFP, whereas EYFP contains the normal Tyr 66 in the fluorophore but is shifted to a yellowish emission by mutation of Thr 203 to Tyr (ref. 9). Both genes have mammalian codon usage and encode appropriate mutations to improve folding[20]. The substitution of ECFP for EBFP shifted the excitation peak from 381 to 433 nm and improved the brightness, signal-to-noise ratio and duration of recording, yet decreased potential concerns regarding autofluorescence, photodamage and incompatibility with caged compounds. The 'yellow cameleons' incorporating ECFP and EYFP have three minor disadvantages. The maximal ratio changes (Fig. 2d) are slightly smaller (~1.5-fold) than for the original EBFP/EGFP cameleons (1.8-fold), perhaps because the emission spectrum of ECFP encroaches more on the EYFP emission. Yellow cameleons are perturbed by acidification below pH 7.0, which mimics a fall in Ca^{2+}. Also, EYFP can undergo reversible photochromism if illuminated too strongly (A. Miyawaki and J. Llopis, unpublished observations). Other properties, such as Ca^{2+} affinities, as well as the qualitative behaviour inside cells, seem to be the same for the two families of cameleons.

When yellow cameleon-2 was transfected into HeLa cells, the fluorescence was uniformly distributed in the cytosolic compartment but excluded from the nucleus (Fig. 3a), as expected for a 74 kDa protein without targeting signals. The time course of the spatially averaged yellow : cyan emission ratios from a single HeLa cell expressing yellow cameleon-2 is shown in Fig. 3b. A submaximal dose of histamine (0.5 μM) produced a significant increase in the emission ratio indicating an initial peak of about 3 μM cytosolic free Ca^{2+}, $[Ca^{2+}]_c$. This response was gradually converted into oscillations and eventually desensitized altogether. However, ATP added as a purinergic agonist could still stimulate another increase in $[Ca^{2+}]_c$ of similar amplitude to the initial histamine response. These responses agree well with the known behaviour of HeLa cells to histamine and ATP[21,22]. Application of the Ca^{2+} ionophore ionomycin followed by a high concentration (20 mM) of extracellular Ca^{2+} gave a large increase in the ratio, which should correspond to the maximal ratio R_{max}. To establish the minimal ratio R_{min}, as required for a simple *in situ* calibration, the cell was loaded with the permeant chelator ester BAPTA/AM, and external Ca^{2+} was clamped to zero with EGTA in the presence of ionomycin. The ratio R_{max}/R_{min} inside cells was about 1.6, equal or slightly greater than that observed *in vitro*. This correspondence argues that the indicator in cells behaved in reasonable accord with its *in vitro* calibration, and that the calibration protocol effectively achieved saturating and zero $[Ca^{2+}]_c$.

Cameleons should be readily directable to interesting sites by fusion to appropriate organellar targeting signals or localized host proteins. For example, addition of a nuclear localization signal to cameleon-2 yielded a Ca^{2+} indicator, 'cameleon-2nu' (Fig. 1c), fluorescence of which was tightly localized to nuclei (Fig. 3c, d) but excluded from nucleoli. The time course of nuclear $[Ca^{2+}]$ proved generally similar to those of $[Ca^{2+}]_c$, confirming previous comparisons of nuclear and cytosolic aequorin[23]. We also succeeded in monitoring agonist-induced changes in the free Ca^{2+} inside the endoplasmic reticulum ($[Ca^{2+}]_{er}$) in individual, intact, non-perfused cells. Two low-affinity indicators, yellow cameleon-3er and 4er (for endoplasmic reticulum) (Fig. 1c), whose Ca^{2+} responses should correspond to the filled circles and open triangles respectively of Fig. 2b, were engineered to reside in the lumen of

endoplasmic reticulum (ER) by addition of a signal sequence at the N terminus and a KDEL signal for ER retention at the C terminus[24]. Reticular patterns of fluorescence were seen in HeLa cells expressing the protein (Fig. 3e). Targeting to the ER was verified by electron-microscopic immunogold localization (Fig. 3f), which showed that almost all of the GFP immunoreactivity was within the ER and nuclear envelope. A few percent of gold particles were in the intermediate compartment between ER and Golgi, but the Golgi apparatus itself was essentially devoid of immunoreactivity. $[Ca^{2+}]_{er}$ reported by yellow cameleon-3er in two neighbouring cells is shown in Fig. 3g. In one cell (filled circles), the indicator was initially saturated ($[Ca^{2+}]_{er} > 100\,\mu M$), as shown by an emission ratio matching R_{max} and a time delay in response to the Ca^{2+}-mobilizing effect of histamine. The agonist eventually depleted $[Ca^{2+}]_{er}$ to about 30 μM, within the dynamic range of the indicator. In the other cell (open circles), $[Ca^{2+}]_{er}$ started at about 60 μM and responded to histamine with much less time delay, soon levelling off at 1.5 μM. The depletion of $[Ca^{2+}]_{er}$ was promptly reversed by a histamine antagonist, cyproheptadine, and recapitulated by ATP. Responses to thapsigargin blockage of the ER Ca^{2+}-ATPase were also heterogeneous, whereas ionomycin immediately clamped $[Ca^{2+}]_{er}$ almost to zero. To measure resting $[Ca^{2+}]_{er}$ values above 100 μM, we turned to the lowest-affinity indicator, yellow cameleon-4er (Figs 2b and 3h). This variant was clearly not saturated, because the ratio started well below R_{max}, fell immediately upon histamine stimulation, but was delayed in recovering after antagonist application. Combined results from the two indicators separately applied to 75 cells showed $[Ca^{2+}]_{er}$ ranging from 60 to 400 μM before and 1 to 50 μM after application of a maximal dose of agonists. Our estimates for basal $[Ca^{2+}]_{er}$ fall roughly in the middle of previous estimates, which range from 1 to 2,000 μM (refs 11, 14, 15, 25). Previous measurements using small-molecule indicators are subject to severe uncertainties in dye localization and Mg^{2+} interference. Aequorin experiments can only be done on cell populations and are complicated by the opposing abilities of Ca^{2+} both to stimulate light output and to irreversibly destroy the indicator. ER-targeted cameleons avoid both sets of problems. Ca^{2+} stores in the ER have recently been suggested to contain spatially and functionally distinct compartments[13,26]. Cameleons fused to different ER sequences should be able to examine such heterogeneity with the unique combination of precise molecular targeting, single-cell physiological imaging, and ultrastructural localization.

Is FRET between GFPs limited to detecting intramolecular proximity, or can it also detect intermolecular associations? Yellow cameleon-2 was expressed as two separate pieces: ECFP–calmodulin and M13–EYFP (Fig. 1c). When these two proteins were mixed *in vitro*, the spectral difference between zero and saturating Ca^{2+} was similar to but somewhat larger than that for the corresponding intramolecular association in the fully fused construct (data not shown), presumably because the unfused partners could get much further apart from each other in the absence of Ca^{2+}. When expressed in HeLa cells, ECFP–calmodulin and M13–EYFP were distributed throughout both the cytoplasm and the nucleus, as would be expected from their molecular weights (M_r 44K and 30K, respectively). This pattern is quite different from the exclusion of intact yellow cameleon-2 from the nucleus. Histamine mobilization of Ca^{2+} elevated the emission ratio of EYFP to ECFP in both cytoplasm and nucleus, an effect reversed by a histamine antagonist (Fig. 4, circles). ATP caused a similarly reversible increase in the ratio. Such physiological $[Ca^{2+}]_c$ transients caused reciprocal changes in the EYFP and ECFP intensities (Fig. 4, lines without symbols), as expected for association/dissociation effects on FRET, whereas artefacts such as a change of focus caused parallel changes that were cancelled by calculating the ratios. Thus GFP-based FRET can monitor the dynamics of reversible heterodimerizaiton in live cells. In a recent alternative approach[27], blue- and green-emitting GFPs were linked through the calmodulin-binding domain of smooth-muscle myosin light-chain kinase. FRET between the GFPs was disrupted *in vitro* upon binding of unlabelled $(Ca^{2+})_4$-calmodulin to the linker. The fusion protein was introduced into cells only by microinjection, and showed small fluorescence response to $[Ca^{2+}]_c$ that were amplifiable by co-injection of exogenous calmodulin.

Many further improvements in cameleons should be possible by mutagenesis, whereas small-molecule indicators can only be optimised by more laborious chemical resynthesis. The targetability of

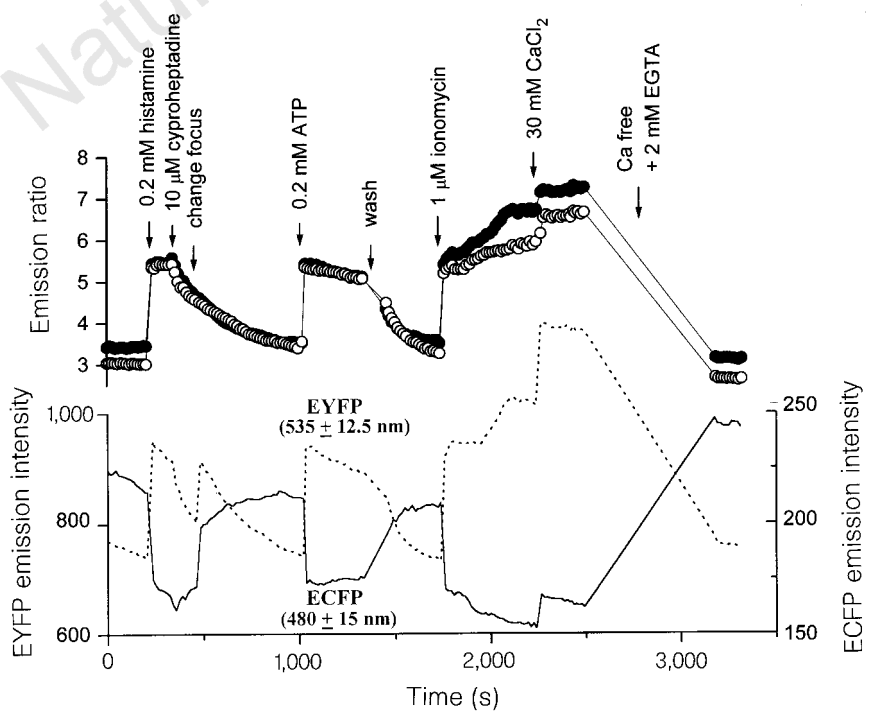

Figure 4 GFP-based detection of protein association/dissociation. Top, 535 to 480 nm emission ratios (filled and open circles) in two adjacent cells co-transfected with M13–EYFP and ECFP–calmodulin. Bottom, 535 (broken line, left-hand scale) and 480 nm (solid line, right-hand scale) emissions, background-corrected, from the cell corresponding to the filled circles.

cameleons may eventually allow Ca^{2+} measurements at previously inaccessible sites, such as the immediate vicinity of synaptic vesicles or Ca^{2+} channels. Cameleons should be well suited to genetically tractable organisms such as bacteria, yeast, nematodes, flies, plants and transgenic mice. Fluorescent indicators for analytes other than Ca^{2+} might be engineered by sandwiching other conformationally responsive receptors between GFP donors and acceptors. Fluorescence readout of intermolecular associations by FRET (as in Fig. 4) is non-destructive, quantifiable with high spatiotemporal resolution, and probably applicable to any compartment of the cell and to many proteins other than calmodulin and M13. However, the ratio of intensities in the acceptor and donor channels starts from a non-zero baseline even in the absence of FRET. Therefore, rare associations will be hard to detect, and positive and negative controls are crucial, such as the ability to switch the putative association on and off, ideally *in situ*. The dynamic range of such measurements both of Ca^{2+} and of protein association will benefit from further improvements in the GFP mutants to reduce leakage of the donor emission into the acceptor emission band. □

Methods

Gene construction. The cDNA of the GFP blue mutant Y66H/Y145F (ref. 1) was amplified by the polymerase chain reaction (PCR) with a sense primer containing a *Bam*HI site and a reverse primer containing an *Sph*I site and eliminating the GFP stop codon. Similarly the cDNA of S65T was amplified with a *Sac*I site and an *Eco*RI site introduced to the 5′ and 3′ ends of the gene, respectively. Two restriction sites (*Sph*I and *Sac*I) were introduced by PCR into the 5′ and 3′ ends of the calmodulin–M13 gene, respectively, using pHY1 (ref. 16) as a template. The restricted products were ligated and cloned in-frame into the *Bam*HI/*Eco*RI sites of pRSETB (Invitrogen). The modifications of the boundary regions between Y66H/Y145F and calmodulin and between M13 and S65T were performed by PCR or by a combined use of restriction enzymes, Klenow fragment of DNA polymerase I, T4 DNA polymerase, mung-bean exonuclease, and T4 DNA ligase. Enhanced GFP mutants EBFP, ECFP and EYFP were created by introducing appropriate substitutions[2,9] into the commercially available phEGFP plasmid from Clontech, which has mammalian codon usage[20] and mutations F64L and S65T. Oligonucleotide-directed mutageneses were performed using the Muta-Gene Phagemid *in vitro* kit (Bio-Rad). The 5′ end of the EBFP or ECFP gene was modified by PCR to have a *Hin*dIII restriction site followed by a Kozak consensus sequence[28] (ACCGCC-ATG). The *Hin*dIII/*Eco*RI fragment encoding the entire chimaeric protein was subcloned in the mammalian expression vector pcDNA3 (Invitrogen). For cameleon-2nu, the cameleon-2 cDNA was extended by PCR at the 3′ end with the sequence encoding the nuclear localization signal (PKKKRKVEDA). Yellow cameleon-3er and -4er cDNA were obtained by extending yellow cameleon-3 cDNA at the 5′ end with the sequence encoding the signal peptide from calreticulin (MLLSVPLLLGLLGLAAAD), and at the 3′ end with the sequence encoding the ER retention signal (KDEL)[24]. The cDNAs coding for ECFP–calmodulin and M13–EYFP were obtained from yellow cameleon-2 by PCR and cloned into pRSETB behind a polyhistidine tag for bacterial expression and into pcDNA3 behind a Kozak sequence for mammalian expression.

Protein expression, *in vitro* spectroscopy, Ca^{2+} titrations, and reaction kinetics. Chimaeric proteins were expressed in *Escherichia coli*, purified and spectroscopically characterized as previously described[2]. Ca^{2+} titrations were performed by reciprocal dilution of Ca^{2+}-free and Ca^{2+}-saturated buffers[10]. *In situ* calibration for $[Ca^{2+}]$ used the equation[29] $[Ca^{2+}] = K'_d[(R - R_{min})/(R_{max} - R)]^{(1/n)}$, where K'_d is the apparent dissociation constant corresponding to the Ca^{2+} concentration at which R is midway between R_{max} and R_{min}, and n is the Hill coefficient. Fast kinetic experiments were performed in a stopped-flow spectrofluorometer (Applied Photophysics). After rapid mixing of purified cameleon-1/E104Q (0.8 μM final concentration) and Ca^{2+} of various concentrations in 20 mM MOPS, 100 mM KCl, pH 7.2, at 25 °C, the fluorescence was monitored using an excitation wavelength of 380 nm with an emission cut-on filter of 500 nm. The observed first-order constant (k_{obs}) was calculated from each averaged set of data by nonlinear regression analysis.

Electron microscopy and immunolabelling. Immunogold labelling of ultrathin sections was performed as described previously[30]. The polyclonal antibody against GFP was a gift from C. Zuker (University of California, San Diego).

Imaging. Between 2 and 5 days after cDNA transfection with lipofectin (Gibco BRL), HeLa cells at 22 °C were imaged on a Zeiss Axiovert microscope with a cooled CCD camera (Photometrics, Tucson, AZ), controlled by MetaFluor 2.75 software (Universal Imaging, West Chester, PA). Dual-emission ratio imaging of yellow cameleons used a 440DF20 excitation filter, a 455DRLP dichroic mirror, and two emission filters (480DF30 for ECFP, 535DF25 for EYFP) alternated by a filter changer (Lambda 10-2, Sutter Instruments, San Rafael, CA). Interference filters were obtained from Omega Optical and Chroma Technologies (Brattleboro, VT).

Received 8 May; accepted 24 June 1997.

1. Heim, R., Prasher, D. C. & Tsien, R. Y. Wavelength mutations and post-translational autoxidation of green fluorescent protein. *Proc. Natl Acad. Sci. USA* **91,** 12501–12504 (1994).
2. Heim, R. & Tsien, R. Y. Engineering green fluorescent protein for improved brightness, longer wavelengths and fluorescence energy transfer. *Curr. Biol.* **6,** 178–182 (1996).
3. Crivici, A. & Ikura, M. Molecular and structural basis of target recognition by calmodulin. *Annu. Rev. Biophys. Biomol. Struct.* **24,** 85–116 (1995).
4. Babu, Y. S., Bugg, C. E. & Cook, W. J. Structure of calmodulin refined at 2.2 Å resolution. *J. Mol. Biol.* **204,** 191–204 (1988).
5. Falke, J. J., Drake, S. K., Hazard, A. L. & Peersen, O. B. Molecular tuning of ion binding to calcium signaling proteins. *Q. Rev. Biophys.* **27,** 219–290 (1994).
6. Ikura, M. *et al.* Solution structure of a calmodulin-target peptide complex by multidimensional NMR. *Science* **256,** 632–638 (1992).
7. Heim, R., Cubitt, A. B. & Tsien, R. Y. Improved green fluorescence. *Nature* **373,** 663–664 (1995).
8. Cormack, B. P., Valdivia, R. H. & Falkow, S. FACS-optimized mutants of the green fluorescent protein (GFP). *Gene* **173,** 33–38 (1996).
9. Ormö, M. *et al.* Crystal structure of the *Aequorea victoria* green fluorescent protein. *Science* **273,** 1392–1395 (1996).
10. Grynkiewicz, G., Poenie, M. & Tsien, R. Y. A new generation of Ca^{2+} indicators with greatly improved fluorescence properties. *J. Biol. Chem.* **260,** 3440–3450 (1985).
11. Tse, F. W., Tse, A. & Hille, B. Cyclic Ca^{2+} changes in intracellular stores of gonadotropes during gonadotropin-releasing hormone-stimulated Ca^{2+} oscillations. *Proc. Natl Acad. Sci. USA* **91,** 9750–9754 (1994).
12. Hofer, A. M. & Schulz, I. Quantification of intraluminal free [Ca] in the agonist-sensitive internal calcium store using compartmentalized fluorescent indicators: some considerations. *Cell Calcium* **20,** 235–242 (1996).
13. Golovina, V. A. & Blaustein, M. P. Spatially and functionally distinct Ca^{2+} stores in sarcoplasmic and endoplasmic reticulum. *Science* **275,** 1643–1648 (1997).
14. Montero, M. *et al.* Monitoring dynamic changes in free Ca^{2+} concentration in the endoplasmic reticulum of intact cells. *EMBO J.* **14,** 5467–5475 (1995).
15. Kendall, J. M., Badminton, M. N., Sala-Newby, G. B., Campbell, A. K. & Rembold, C. M. Recombinant apoaequorin acting as a pseudo-luciferase reports micromolar changes in the endoplasmic reticulum free Ca^{2+} of intact cells. *Biochem. J.* **318,** 383–387 (1996).
16. Porumb, T., Yau, P., Harvey, T. S. & Ikura, M. A calmodulin-target peptide hybrid molecule with unique calcium-binding properties. *Protein Eng.* **7,** 109–115 (1994).
17. Maune, J. F., Klee, C. B. & Beckingham, K. Ca^{2+} binding and conformational change in two series of point mutations to the individual Ca^{2+}-binding sites of calmodulin. *J. Biol. Chem.* **267,** 5286–5296 (1992).
18. Gao, Z. H. *et al.* Activation of four enzymes by two series of calmodulin mutants with point mutations in individual Ca^{2+} binding sites. *J. Biol. Chem.* **268,** 20096–20104 (1993).
19. Martin, S. R. *et al.* Spectroscopic characterization of a high-affinity calmodulin-target peptide hybrid molecule. *Biochemistry* **35,** 3508–3517 (1996).
20. Zolotukhin, S., Potter, M., Hauswirth, W., Guy, J. & Muzyczka, N. A "humanized" green fluorescent protein cDNA adapted for high levels of expression in mammalian cells. *J. Virol.* **70,** 4646–4654 (1996).
21. Smit, M. J. *et al.* Extracellular ATP elevates cytoplasmatic free Ca^{2+} in HeLa cells by the interaction with a 5′-nucleotide receptor. *Eur. J. Pharmacol.* **247,** 223–226 (1993).
22. Bootman, M. D., Cheek, T. R., Moreton, R. B., Bennett, D. L. & Berridge, M. J. Smoothly graded Ca^{2+} release from inositol 1,4,5-trisphosphate-sensitive Ca^{2+} stores. *J. Biol. Chem.* **269,** 24783–24791 (1994).
23. Brini, M., Marsault, R., Bastianutto, C., Pozzan, T. & Rizzuto, R. Nuclear targeting of aequorin. A new approach for measuring nuclear Ca^{2+} concentration in intact cells. *Cell Calcium* **16,** 259–268 (1994).
24. Kendall, J. M., Dormer, R. L. & Campbell, A. K. Targeting aequorin to the endoplasmic reticulum of living cells. *Biochem. Biophys. Res. Commun.* **189,** 1008–1016 (1992).
25. Bygrave, F. L. & Benedetti, A. What is the concentration of calcium ions in the endoplasmic reticulum? *Cell Calcium* **19,** 547–551 (1996).
26. Button, D. & Eidsath, A. Aequorin targeted to the endoplasmic reticulum reveals heterogeneity in luminal Ca^{++} concentration and reports agonist- or $InsP_3$-induced release of Ca^{++}. *Mol. Biol. Cell* **7,** 419–434 (1996).
27. Romoser, V. A., Hinkle, P. M. & Persechini, A. Detection in living cells of Ca^{2+}-dependent changes in the fluorescence emission of an indicator composed of two green fluorescent protein variants linked by a calmodulin-binding sequence. *J. Biol. Chem.* **272,** 13270–13274 (1997).
28. Kozak, M. The scanning model for translation: an update. *J. Cell Biol.* **108,** 229–241 (1989).
29. Adams, S. R., Bacskai, B. J., Taylor, S. S. & Tsien, R. Y. *Fluorescent Probes for Biological Activity of Living Cells–A Practical Guide* (ed. Mason, W. T.) 133–149 (Academic, New York, 1993).
30. Balch, W. E., McCaffery, J. M., Plutner, H. & Farquhar, M. G. Vesicular stomatitis virus glycoprotein is sorted and concentrated during export from the endoplasmic reticulum. *Cell* **75,** 841–852 (1994).

Acknowledgements. We thank S. R. Adams and A. B. Cubitt for advice, C. Zuker for the GFP antibody, and C. Klee for the original *Xenopus* calmodulin gene. This work was supported by HHMI (R.Y.T.), NIH (R.Y.T.), HFSP (R.Y.T. and A.M.), MRCC (M.I.) and the Spanish Ministry of Science (J.L.). M.I. is an HHMI international research scholar and MRCC scholar.

Correspondence and requests for materials should be addressed to R.Y.T.